JOURNAL OF MATERIALS SCIENCE 32 (1997) 2275–2282

Measurement and analysis of elastic and anelastic properties of alumina and silicon carbide

A. WOLFENDEN
Advanced Materials Laboratory, Mechanical Engineering Department, Texas A&M University, College Station, TX 77843-3123, USA

Measurements of dynamic Young's modulus, E, and damping as a function of temperature, T, were made for alumina and silicon carbide. The Young's modulus data were compared with some from the literature, and analysed in terms of a theoretical framework relating the Debye temperature, θ_D, with the elastic constants. For both materials this analysis yielded a ratio T_0/θ_D which was near 0.4, where T_0 is an empirical fitting constant for the plot of $(E(0) - E)/T$ versus $1/T$ ($E(0)$ is the value of E at 0 K). The analysis of the damping data in terms of an Arrhenius type dependence led to effective activation energies near kT, where k is Boltzmann's constant.

1. Introduction

The elastic properties of ceramics have a wide range of applications for basic research and are important for technological applications. They offer opportunities for a direct measurement of the strength of interatomic bonds; they are pertinent to the theoretical strength of crystals; they are interrelated with specific heat, thermoelastic stresses, expansion coefficients, lattice dynamics and properties of point defects and dislocations. For design in engineering, the elastic moduli are needed for calculations of stress and strain for static or dynamic loading conditions. The elastic properties are needed also in the design of transducers, such as those used in non-destructive testing. Regarding the elastic modulus of a material as a complex term (in the mathematical sense), it is noted that the real part (i.e. the elastic part) of the modulus is the Young's or shear modulus, while the imaginary part of the modulus is the anelastic component, usually termed the damping. The damping of a material controls the rate at which vibrations are dissipated and is obviously of technological interest. For basic research, measurements of damping can provide information on the mechanisms by which point defects, dislocations or interfaces dissipate vibrational energy.

In this paper, the results of measurements of dynamic Young's modulus, E, and damping, Q^{-1}, as a function of temperature, T, for alumina and silicon carbide are presented, compared with some data from the literature, and analysed in terms of a theoretical framework, part of which dates back to Einstein's [1, 2] original relationship between the characteristic frequency of a material and its compressibility (i.e. the relation between the Debye temperature, θ_D, and the elastic constants). For both materials the analysis of the values of Young's modulus yields a ratio T_0/θ_D which is near 0.4, where T_0 is an empirical fitting constant for the plot of $(E(0) - E)/T$ versus $1/T$ ($E(0)$ is the value of E at 0 K). The analysis of the damping data in terms of an Arrhenius type dependence leads to effective activation energies near kT, where k is Boltzmann's constant.

2. Materials and experimental procedure

2.1. Materials

Alumina rods of purity 99.8% and diameter 3.2 mm were obtained from the McDanel Refractory Company. The silicon carbide was obtained from the Norton Company and is known as NC 203. Specimens of alumina were cut to lengths near 25 mm, and specimens of SiC were cut to a size of 50 mm × 4 mm × 3 mm, in both cases with a diamond cut-off saw. The ends of the specimens were made flat and parallel by polishing with a series of SiC papers.

2.2. Experimental procedure

The use of the PUCOT (piezoelectric ultrasonic composite oscillator technique) for measurements of dynamic Young's modulus and damping requires that the mass density (ρ) of the materials be determined. The density of each specimen at room temperature was found by the Archimedes technique. The values of density for high temperatures were adjusted by use of the coefficients of expansion of the specimen materials.

The PUCOT consisted of two α-quartz piezoelectric crystals of the same frequency, glued together with cyanoacrylate glue and attached to a jig. For the specimens of alumina, a frequency of 200 kHz was suitable, while for the SiC specimens a frequency of 120 kHz was used. The drive crystal (D) and the gauge crystal (G) were connected electrically to a closed loop crystal driver, and the gauge crystal was connected

also to a frequency counter. The crystal driver provided an alternating drive voltage (V_d) to excite the crystals to resonance with a standing wave in the longitudinal mode. The gauge crystal detected the response of the vibration as a voltage V_g. The resonant period τ_{DG} of the crystals was measured with the frequency counter. For measurements of Young's modulus (E) and damping (Q^{-1}) at room temperature, the specimen (S) of resonant length (L_s) was glued with cyanoacrylate glue to the bottom of the gauge crystal, the system was adjusted to resonate, and the values of V_d, V_g and τ_{DGS} (the resonant period of the DGS combination) were noted. From the masses (m) of the various components in the system (m_{DG} and m_S), the voltages V_d and V_g, the periods τ_{DG} and τ_{DGS}, L_s and ρ, the values of E, Q^{-1} and strain amplitude were determined. In all cases the strain amplitude was near 10^{-7} and was well within the elastic region of the stress–strain curve for the materials.

For measurements of E and Q^{-1} at elevated temperature, it was necessary to tune a series of fused quartz spacer rods (Q) to resonate at the appropriate frequency and temperatures, i.e. to choose the length of the spacer rod such that $\tau_{DGQ} = \tau_{DG}$ at the temperature of interest. The spacer rod was attached to the bottom of the gauge crystal with cyanoacrylate glue for the tuning. After the tuning process, the specimen was attached to the bottom of the spacer rod with a ceramic glue, the glue was allowed to dry for 24 h, and the DGQS assembly was positioned vertically over the tube furnace such that the specimen was near the middle of the furnace and part of the rod was in the furnace, and the crystals were above the top of the furnace. The crystals were maintained at room temperature by a small electric fan. Finally, the system was adjusted for resonance, and the values of V_d, V_g and τ_{DGQS} were noted. From the masses of the various components in the system (m_{DG}, m_{DGQ}, m_{DGQS} with ceramic glue, and m_S), the voltages V_d and V_g, the periods τ_{DG} and τ_{DGQS}, the expansion coefficient, L_s (corrected by the use of the expansion coefficient) and ρ, the values of E, Q^{-1} and strain amplitude were determined for temperature T. Experiments were carried out at temperatures up to 1473 and 1322 K for the alumina and SiC, respectively. Further details of the PUCOT are given elsewhere [3, 4].

3. Results and discussion

3.1. Young's modulus

The measured values of the dynamic Young's modulus, E, and the mechanical damping, Q^{-1} as a function of temperature, T, are presented in Table I. Plots of E versus T for alumina and silicon carbide are shown in Figs 1 and 2, respectively. The data in Fig. 1 have been fitted to a parabola while those in Fig. 2 have been fitted to a straight line. The equations and correlation coefficients, R, arising from the regression analyses are given in Table II. Plots of E versus T for alumina taken from the paper by Fukuhara and Yamauchi [5] (referred to as FY) and from the paper by Wachtman *et al.* [6] (referred to as W *et al.*) are presented in Figs 3 and 4, respectively. In both of these figures the data have been fitted to parabolas. The results of these regression analyses appear in Table II also. The correlation coefficients fall in the range -0.972 to -0.986. A comparison of the curves in

TABLE I Experimentally determined values of dynamic Young's modulus and damping for Al_2O_3 and SiC

Al_2O_3			SiC		
T (K)	E (GPa)	$10^4 \times Q^{-1}$	T (K)	E (GPa)	$10^4 \times Q^{-1}$
298	436	9	293	450	4.1
613	402	24	633	434	1.4
619	384	9	787	418	15.0
663	379	10	1108	430	34.5
743	380	4	1322	414	125
763	377	4			
1034	363	9			
1073	357	10			
1218	289	244			
1247	283	234			
1293	277	234			
1373	264	92			
1413	256	97			
1449	251	101			
1463	248	103			
1473	246	105			

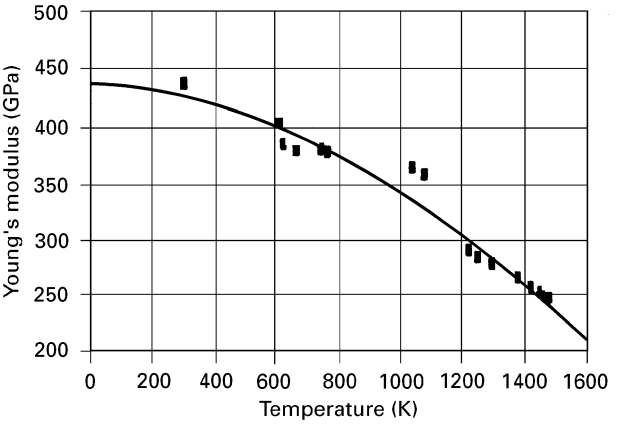

Figure 1 The temperature dependence of Young's modulus for alumina (present data).

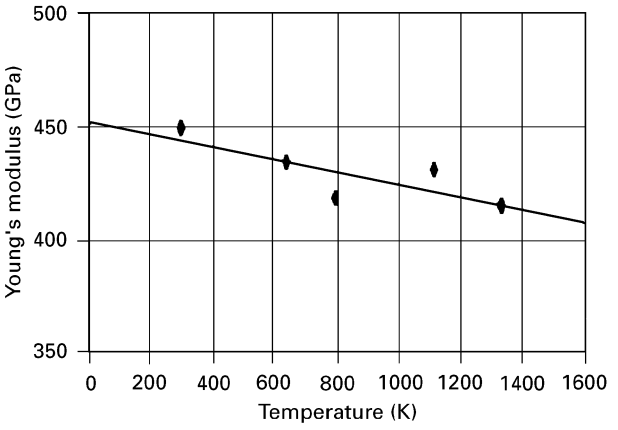

Figure 2 The temperature dependence of Young's modulus for silicon carbide (present data).

TABLE II A listing of the analytical parameters for the curves of E versus T, $(E(0) - E)/T$ versus T^{-1} and Q^{-1} versus T^{-1} for Al_2O_3 and SiC

Al_2O_3				SiC	
			E versus T curves (Figs 1–5)		
Present data:					
$E = 438.4 - 0.01588T - 0.00007926T^2$ (GPa, K)				$E = 453.3 - 0.02913T$	
Correlation coefficient, $R = -0.972$				$R = -0.823$	
From data of FY [5]:				From the data of J *et al.* [7]:	
$E = 410.3 - 0.02341T - 0.000007985T^2$				$E = 406.0 - 0.01429$T	
$R = -0.984$				$R = -0.970$	
From data of W *et al.* [6]:					
$E = 470.7 - 0.01314T - 0.00001713T^2$					
$R = -0.986$					
			$(E(0) - E)/T$ versus T^{-1} curves (Figs 8 – 11, 14 and 15)		
From data of:				From data of:	
	Present	FY [5]	W *et al.* [6]	Present	J *et al.* [7]
$E(0)$(K)	= 438	410	471	453	406
R	= − 0.893	− 0.322	− 0.987	− 0.626	− 0.470
b(GPa K^{-1})	= 0.270	− 0.0331	0.0382	0.0455	0.0161
T_0(K)	= 996	69	256	397	67
			Q^{-1} versus T^{-1} curves (Figs 16–21)		
		Present	From data of FY[5]		Present
All data	R	= − 0.502	− 0.880		− 0.563
	H (eV/atom)	= 0.11	0.08		0.09
RT[a] datum excluded	R	= − 0.631	− 0.954		− 0.824
	H (eV/atom)	= 0.27	0.12		0.43

[a] RT denotes room temperature.

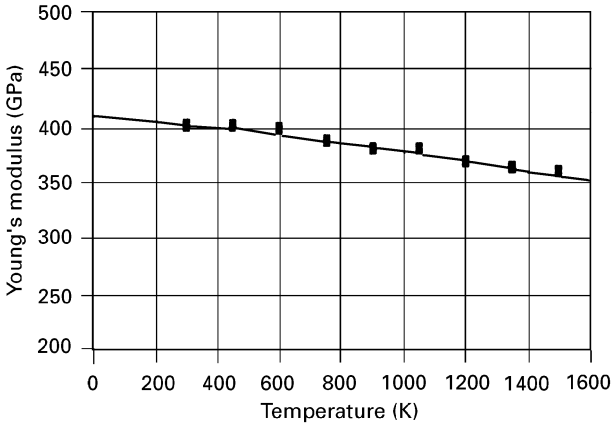

Figure 3 The temperature dependence of Young's modulus for alumina (after FY [5]).

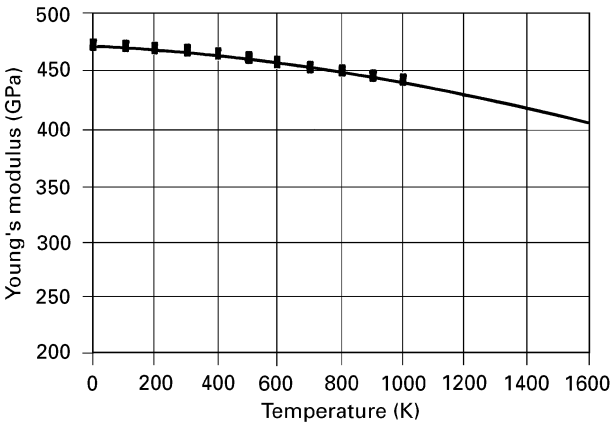

Figure 4 The temperature dependence of Young's modulus for alumina (after W *et al.* [6]).

Figs 1, 3 and 4 reveals that while the values of E near room temperature are near 440 GPa for all three sets of results, at temperatures beyond 1000 K the present data are lower than those of the other two sets. Differences in the measurement techniques and in the purity of the specimen materials may account for this divergence.

A plot of E versus T for SiC from the paper by Jaminet *et al.* [7] (referred to as J *et al.*) is shown in Fig. 5. The data points have been fitted to a straight line, and the equation and the correlation coefficient, R, from the regression analysis are listed in Table II. The values of Young's modulus for the reaction bonded SiC from Coors [7] are roughly 35 GPa lower than those for the NC 203 SiC.

It is interesting to note that the curves of E versus T in Figs 1, 3 and 4 for alumina show a flattening out as the temperature approaches 0 K. The temperature dependence of elastic constants has been discussed in terms of non-linear lattice dynamics by Wachtman [8]. In that discussion it was pointed out that elastic constants vary with temperature because of thermal expansion. This can be attributed to the fact that both elasticity and thermal expansion depend on non-linear terms in the interatomic potential energy. The curves in these figures can be regarded as having a transition

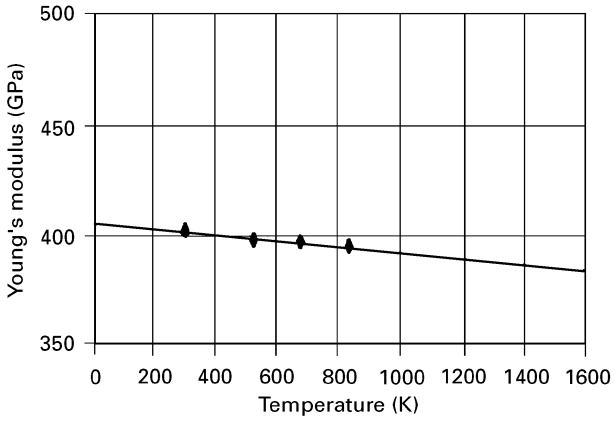

Figure 5 The temperature dependence of Young's modulus for silicon carbide (after J *et al.* [7]).

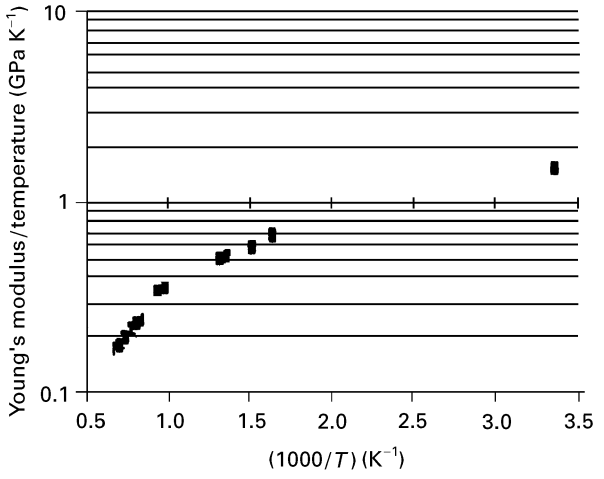

Figure 6 The ratio of Young's modulus to temperature as a function of reciprocal temperature for alumina (present data).

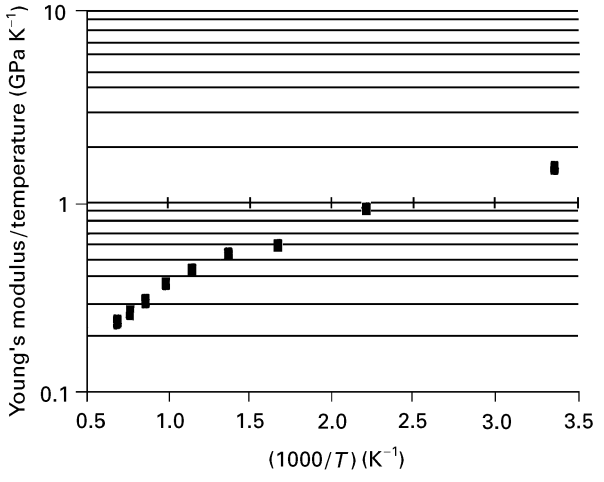

Figure 7 The ratio of Young's modulus to temperature as a function of reciprocal temperature for alumina (after FY [5]).

from zero slope at 0 K to an essentially linear decrease with increasing temperature. Such behaviour would be expected to conform to an equation of this form:

$$E = E(0) - bT\exp(-T_0/T) \quad (1)$$

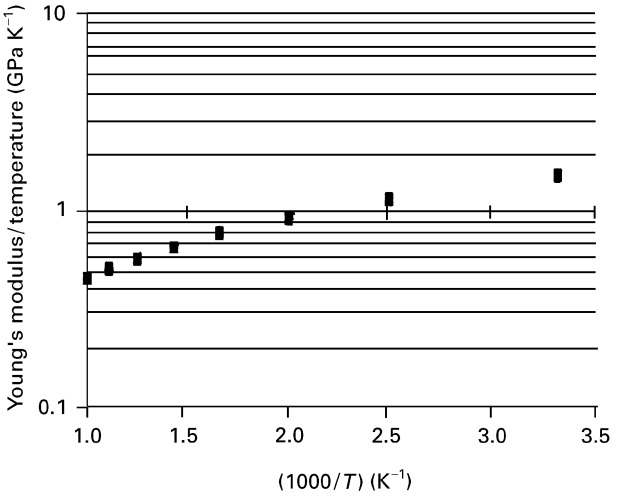

Figure 8 The ratio of Young's modulus to temperature as a function of reciprocal temperature for alumina (after W *et al.* [6]).

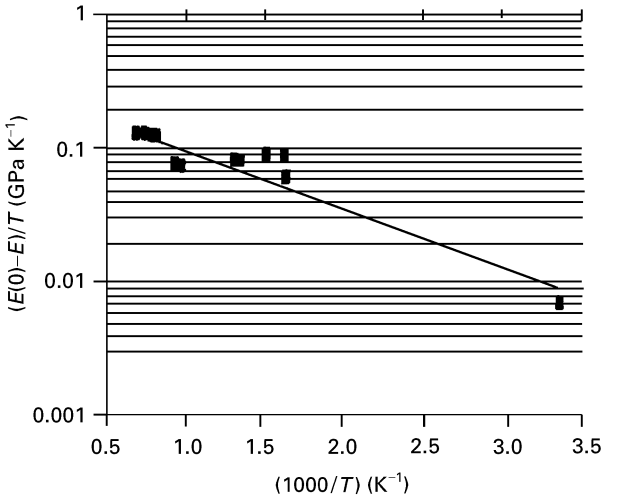

Figure 9 $(E(0) - E)/T$ plotted as a function of reciprocal temperature for alumina, where $E(0) = 438$ GPa.

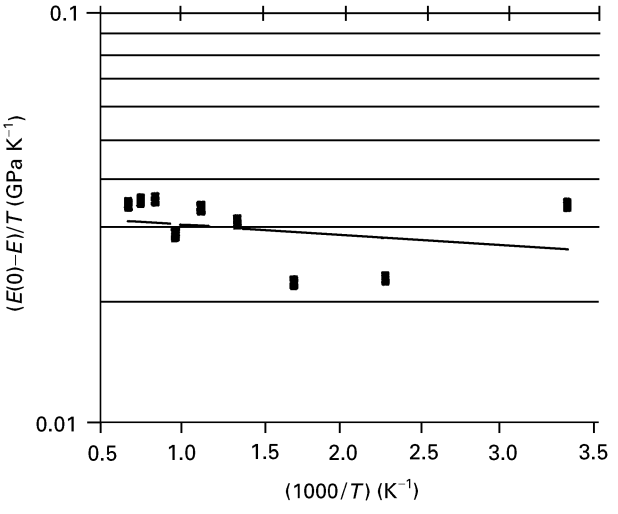

Figure 10 $(E(0) - E)/T$ plotted as a function of reciprocal temperature for alumina, where $E(0) = 410$ GPa (after FY [5]).

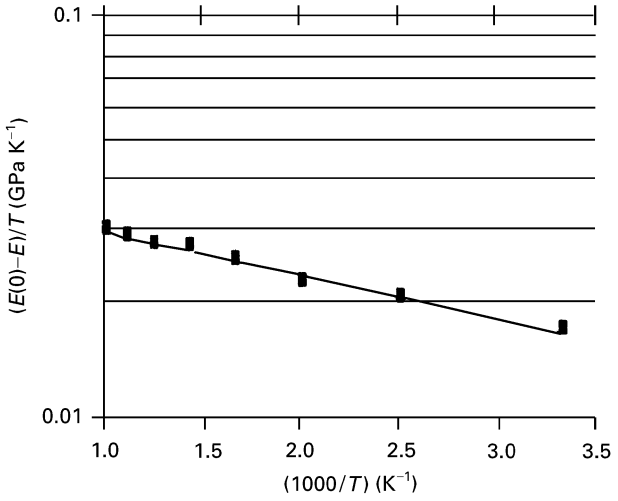

Figure 11 $(E(0) - E)/T$ plotted as a function of reciprocal temperature for alumina, where $E(0) = 471$ GPa (after W *et al.* [6]).

TABLE III Values of the Debye temperature θ_D and the characteristic temperature T_0

Al_2O_3			SiC	
Data source	θ_D (K)	T_0 (K)	θ_D (K)	T_0 (K)
[12–14]	607			
[15]			862	
[16]			903	
[17]			937	
$(ab)^{0.5}$[a]			1196 ± 10	
W *et al.* [6]	1045			
AVG.	826		975	
Present		996		397
Reported		309		
by W *et al.* [6]		312		
From data		69		
of FY [5]				
From data		256		
of W *et al.* [6]				
From data				67
of J *et al.* [7]				
AVG.		388		232
(T_0 AVG/θ_D AVG		0.47		0.24)

[a] a and b are the values of θ_D for Si and C (645 ± 5 and 2219 ± 20 K, respectively) [10].

in which $E(0)$ is the value of Young's modulus at 0 K, and b and T_0 are empirical constants [6]. Anderson [9] showed that for data at high temperatures, T_0 corresponds to approximately half the Debye temperature ($\theta_D/2$).

The analysis of the E versus T data for alumina in the context of Equation 1 started by making plots of (E/T) versus $1/T$ as shown in Figs 6–8 for the present data, and for the data of FY and W *et al.*, respectively. The convergence to linearity at the end of the plot corresponding to the high temperatures is seen clearly in Figs 6 and 7. The analytical procedure continued with plots of $(E(0) - E)/T$ versus $1/T$, as shown in Figs 9–11, where the values of $E(0)$ of 438, 410 and 471 GPa (for the present case, and for the cases of FY and W *et al.*, respectively) were obtained from the results of the regression analyses documented in Table II. The results of the regression analyses of Figs 9–11 are presented also in Table II. The curves in Fig. 9 and 11 fit well to straight lines, with correlation coefficients R of -0.893 and -0.987, respectively. There is more scatter in the data of FY, yielding an R value of -0.322. From the analysis we arrive at the following values for the empirical constants b and T_0: 0.270, 0.0331 and 0.0382 GPa K^{-1}; 996, 69 and 256 K (for the present case, for the cases of FY and of W *et al.*, respectively). Two of the values for b agree quite well, while there is a spread in the values of T_0. The values of T_0 are compiled in Table III along with two values (309 and 312 K) reported by W *et al.* [6]

To complete the analysis of the Young's modulus data for alumina, we need a value for the Debye temperature. Wachtman *et al.* [6] list a value of 1045 K for θ_D. We have calculated a value of θ_D for alumina using the computational method of Wolfenden and Harmouche [11] and the elastic constants reported by Mayer and Hiedemann [12–14]. This calculated value is 607 K. Thus, in Table III we list the average of these two values of the Debye temperature (average = 826 K) and the average of the T_0 values for alumina (average = 388 K), and find that the ratio T_0/θ_D is 0.47. This result agrees well with that found by Anderson [9] for data on oxides at high temperatures.

Corresponding analyses of the present E versus T data and those of Jaminet *et al.* [7] in Figs 2 and 5 for SiC were made. Figs 12 and 13, and 14 and 15 show, respectively, the plots of E/T versus $1/T$ and $(E(0) - E)/T$ versus $1/T$, where the values of $E(0)$ of 453 and 406 GPa were obtained from the regression analyses of Figs 2 and 5. As was the case with the results for alumina, the convergence to linearity at the end of the plot corresponding to the high temperatures is seen in Fig. 12 for SiC. The convergence is not so obvious in Fig. 13. The plots in Figs 14 and 15 have some scatter with a correlation coefficient R of -0.626 and -0.470. The values of b and T_0 to fit with Equation 1 are 0.0455 and 0.0161 GPa K^{-1}, and 397 and 67 K for SiC. Values of the Debye temperature for SiC were calculated two different ways: one calculation was done with the method of Wolfenden and Harmouche [11] using the elastic constants data of Tolpygo [15], Martin [16] and Arlt and Schodder [17]; the other calculation was simply to take the harmonic mean of the θ_D values for Si and C (diamond) listed by Konti and Varshni [10]. The calculated values of the Debye temperature were 862, 903, 937 and 1196 ± 10 K, respectively. These values are tabulated in Table III, along with their average value of 975 K. Thus, the ratio T_0/θ_D is 0.24 for SiC. This result is somewhat smaller than that found by Anderson [9] for elastic modulus data at high temperatures. The smaller result may be due to the restricted number (2) of values for T_0 and to their wide range (397 and 67 K).

3.2. Damping

Plots of Q^{-1} versus T^{-1} on log–linear axes for alumina and silicon carbide are shown in Figs 16 and 17, respectively. The data in these figures have been

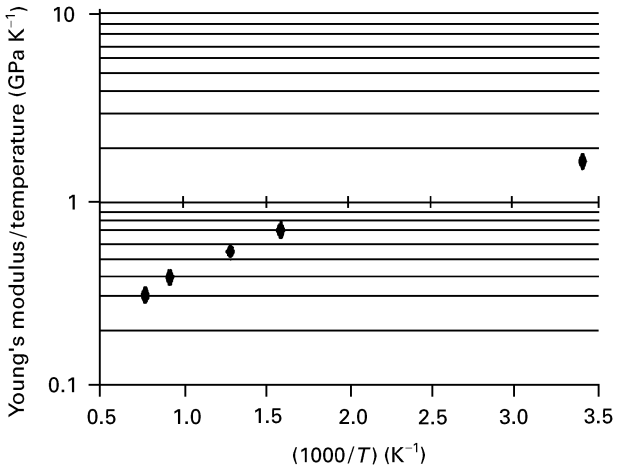

Figure 12 The ratio of Young's modulus to temperature as a function of reciprocal temperature for silicon carbide (present data).

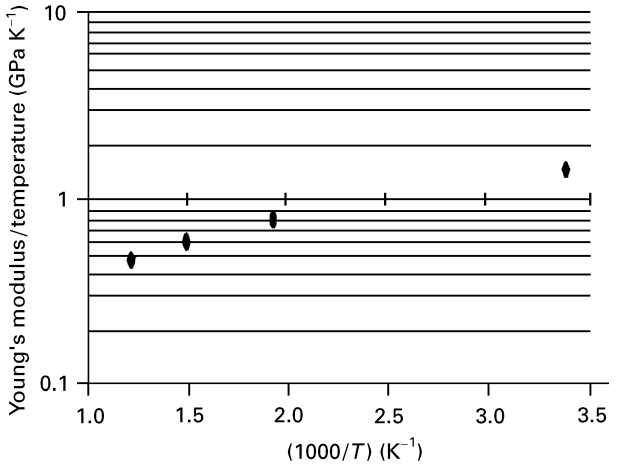

Figure 13 The ratio of Young's modulus to temperature as a function of reciprocal temperature for silicon carbide (data from J *et al.* [7]).

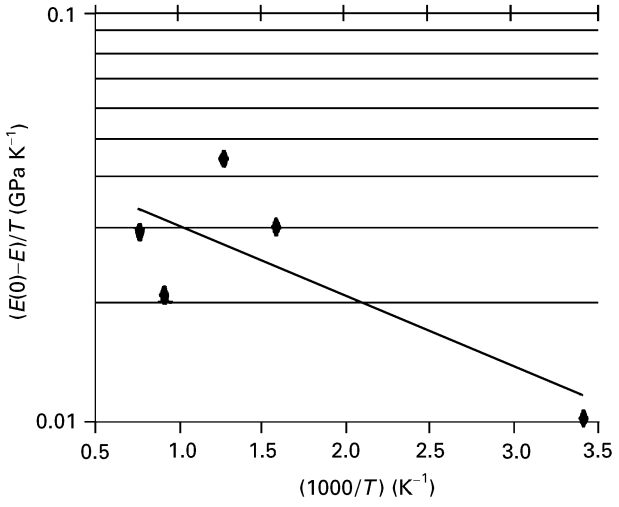

Figure 14 $(E(0) - E)/T$ plotted as a function of reciprocal temperature for silicon carbide, where $E(0) = 453$ GPa (present data).

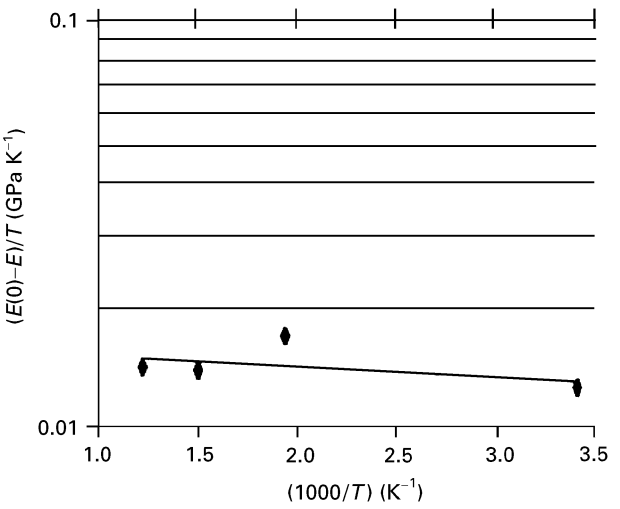

Figure 15 $(E(0) - E)/T$ plotted as a function of reciprocal temperature for silicon carbide, where $E(0) = 406$ GPa (data from J *et al.* [7]).

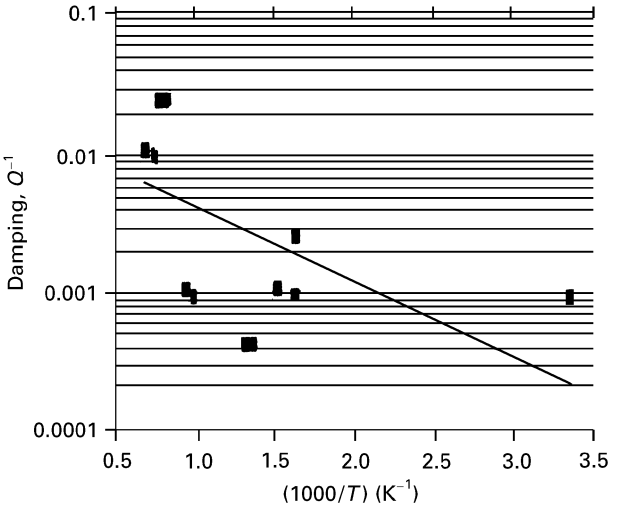

Figure 16 Damping as a function of reciprocal temperature for alumina (present data).

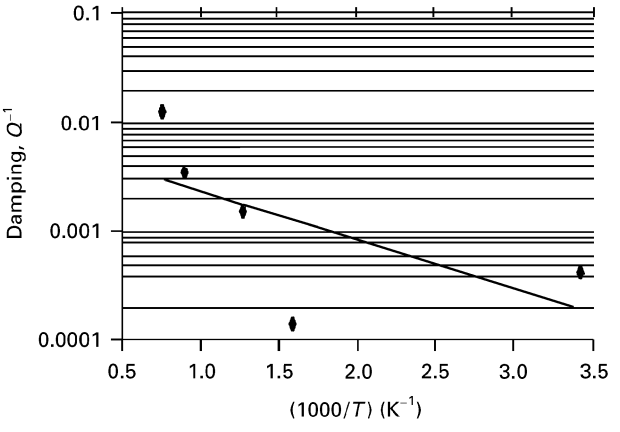

Figure 17 Damping as a function of reciprocal temperature for silicon carbide (present data).

fitted to straight lines. The correlation coefficients, R, arising from the regression analyses are given in Table II, and are -0.502 and -0.563, respectively. Clearly, there is considerable scatter in the data. A plot of Q^{-1} versus T^{-1} for alumina taken from the paper by Fukuhara and Yamauchi [5] is presented in Fig. 18. Again the data have been fitted to a straight line. The result of the regression analysis appears in Table II also. The correlation coefficient is -0.880. A comparison of the values in Figs 16 and 18 reveals that

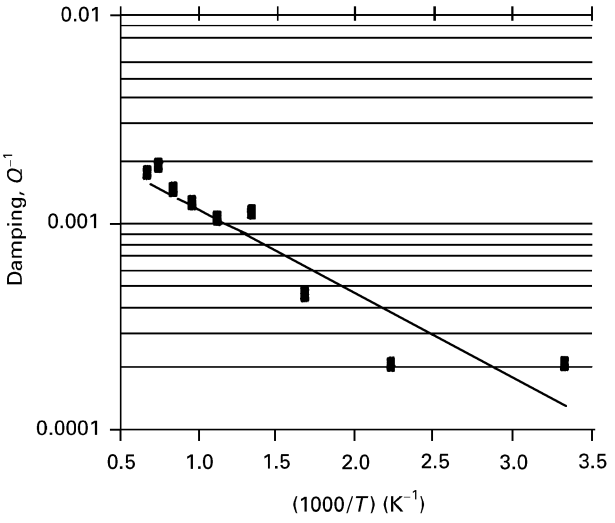

Figure 18 Damping as a function of reciprocal temperature for alumina (data from FY [5]).

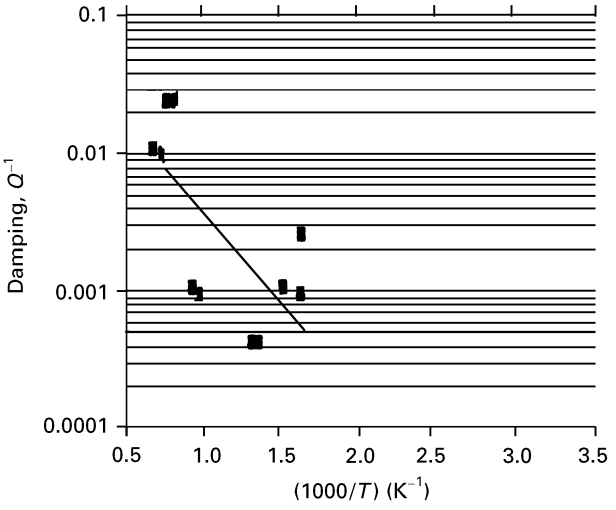

Figure 19 Selected data: damping as a function of reciprocal temperature for alumina (present data).

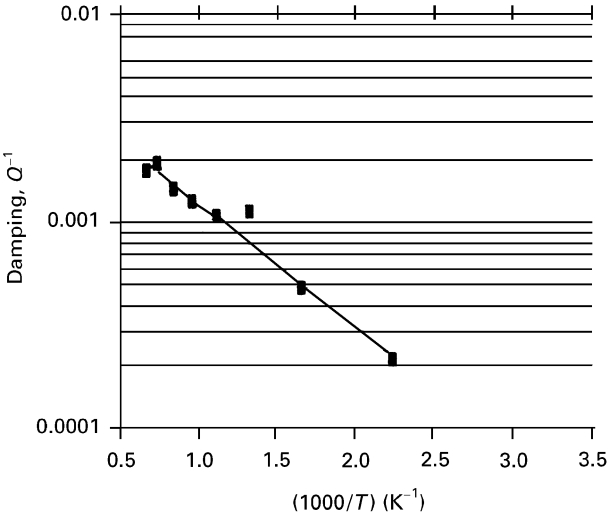

Figure 20 Selected data: damping as a function of reciprocal temperature for alumina (data from FY [5]).

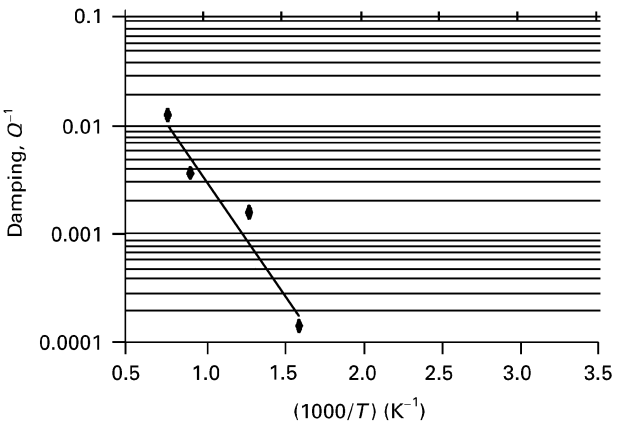

Figure 21 Selected data: damping as a function of reciprocal temperature for silicon carbide (present data).

near room temperature the two sets of data are in close agreement, but at the higher temperatures the data differ by a factor near three. Again, it is likely that differences in the measurement techniques and in the purity of the specimen materials contribute to this divergence.

Following the notion that the elastic properties (Young's modulus) of these ceramic materials can be assessed in terms of high temperature data and low temperature data (see Section 3.1), we have attempted to see if the same division can be applied to the anelastic data, i.e. the damping results. Accordingly, the average value of T_0 for alumina (388 K) has been taken as the temperature for the division of the data. Thus, from Figs 16 and 18 we have deleted the data obtained at room temperature and have reproduced the graphs in Figs 19 and 20. Interestingly, there are improvements in the fits to straight lines for both data sets. The values of R are -0.631 and -0.954, for the present data and for those of FY. A similar treatment has been applied to the data for SiC and the result is displayed in Fig. 21. The temperature for the division of the SiC data was 397 K, and the value of R improved from -0.563 to -0.824. At this stage, the division of the anelastic data in this manner is a purely empirical approach with no physical mechanism behind it.

The damping data can be analysed, however, in a different way to yield information on mechanisms. Thus, the curves in Figs 13–18 have been analysed in terms of an Arrhenius type equation:

$$Q^{-1} = Q^{-1}(0) \exp(-H/kT) \quad (2)$$

where $Q^{-1}(0)$ is a reference value of damping, H is an effective activation energy and k is Boltzmann's constant. The values of H obtained are listed in Table II and lie in the range 0.11–0.27 eV/atom for alumina and 0.09–0.43 eV/atom for SiC. These effective activation energies are low for ceramic systems. For example, the activation energy for diffusion of oxygen in alumina lies in the range 2.5 to 8.2 eV/atom [18, 19] while that for Al in alumina is 4.9 eV/atom [20]; the activation energy for the diffusion of carbon in SiC is near 8 eV/atom [21]. Table IV gives a listing of some diffusion related mechanisms and their associated

TABLE IV Diffusion related mechanisms and their associated activation energies

Mechanism	Activation energy (eV/atom)	Reference
Lattice diffusion in Al_2O_3	5.29	[22]
Sub-boundary diffusion in Al_2O_3	8.81	[22]
Oxygen diffusion in	8.15	[18]
single crystal Al_2O_3	2.50	[19]
Oxygen diffusion in polycrystalline Al_2O_3	4.77	[19]
Al in Al_2O_3	4.94	[20]
Ionic conduction in SiO_2–Na_2O–Al_2O_3–ZrO_2	0.488–0.740	[23]
Na^+ diffusion in Al_2O_3–Na_2O	0.05 (localized jumps) 0.25 (long-range diffusion)	[24]
K^+ and Na^+ diffusion in Al_2O_3–Na_2O–K_2O	0.183–0.387	[25]
C in SiC	7.4–8.2	[21]
High temperature back ground damping	0.025–0.125	[26]
Present results Al_2O_3	0.11–0.27	
SiC	0.09–0.43	

activation energies. Although the present values of H for Al_2O_3 are consistent with the mechanism of impurity ion diffusion (K^+ or Na^+), it seems also likely that for both materials (Al_2O_3 and SiC) the low values of H may reflect a contribution from thermal energy to the damping. The values of kT for temperatures in the range 300 to 1500 K (the range of interest here) are 0.025 to 0.125 eV/atom.

4. Summary

From this study of the measurements of the elastic and anelastic properties of alumina and silicon carbide as a function of temperature, the following main findings hold:

1. Young's modulus (E) values for alumina and SiC fit these equations, respectively:

$$E = 438.4 - 0.01588T - 0.00007926T^2 \quad (298 < T < 1473\ \text{K}) \tag{3}$$

$$E = 453.3 - 0.02913T \quad (293 < T < 1322\ \text{K}) \tag{4}$$

where E is in GPa and T is temperature.

2. The Young's modulus data can be grouped into a high temperature regime and a low temperature regime. Thus, the Young's modulus data for both materials also fit this equation:

$$E = E(0) - bT\exp(-T_0/T) \tag{1}$$

where $E(0)$ is the value of Young's modulus at 0 K, and b and T_0 (the characteristic temperature) are empirical constants, found to be 0.270 GPa K^{-1} and 996 K for alumina, and 0.0455 GPa K^{-1} and 397 K for SiC.

3. The ratio of the characteristic temperature T_0 and the Debye temperature θ_D for both materials was found to be near 0.4.

4. For both materials the effective activation energy for the change in damping with change in temperature was found to be near kT, where k is Boltzmann's constant, reflecting the contribution to the damping from thermal energy. For alumina the value of the effective activation energy was also consistent with the mechanism of impurity ion diffusion (K^+ or Na^+).

5. There may be a possibility of grouping the damping data into a high temperature regime and a low temperature regime.

Acknowledgements

The author is grateful to M. Singh of the NASA Lewis Research Center for his interest in co-operative research on ceramics over many years, to V. K. Kinra, H. R. Thornton, K. T. Hartwig, D. E. Bray and R. E. Goforth for useful discussions, and to P. J. Rynn, P. T. Jaminet, K. A. Oliver and J. E. Kinzy for experimental assistance.

References

1. A. EINSTEIN, *Ann. Physik* **34** (1910) 170.
2. *Idem*, *ibid.* **34** (1910) 590.
3. A. WOLFENDEN and M. R. HARMOUCHE, *J. Mater. Sci.* **28** (1993) 1015.
4. *Idem J. Test. Eval.* **21** (1993) 470.
5. M. FUKUHARA and I. YAMAUCHI, *J. Mater. Sci.* **28** (1993) 4681.
6. J. B. WACHTMAN, Jr., W. E. TEFFT, D. G. LAM, Jr and C. S. APSTEIN, *Phys. Rev.* **122** (1961) 1754.
7. P. T. JAMINET, A. WOLFENDEN and V. K. KINRA, M^3D: Mechanics and Mechanisms of Material Damping, ASTM STP 1169, edited by V. K. Kinra and A. Wolfenden, (American Society for Testing and Materials, Philadelphia, 1992) pp. 432–446.
8. J. B. WACHTMAN, Jr, in Mechanical and Thermal Properties of Ceramics, Proceedings of the Symposium, Gaithersburg, MD, 1–2 April, 1968, National Bureau of Standards Special Publ. 303 (National Bureau of Standards, Washington, May 1969) pp. 139–168.
9. O. L. ANDERSON, Phys. Rev. **144** (1966) 553.
10. A. KONTI and Y. P. VARSHNI, Canadian *J. Phys.* **47** (1969) 2021.
11. A. WOLFENDEN and M.R. HARMOUCHE, *J. Appl. Phys.* **72** (1992) 2732.
12. W. G. MAYER and E. A. HIEDEMANN, *J. Acoust. Soc. Amer.* **30** (1958) 756.
13. *Idem*, *ibid.* **32** (1960) 1699.
14. *Idem*, *Acta Crystallogr* **14** (1961) 323..
15. K. B. TOLPYGO, *Fiz. Tverd. Tela* **2** (1960) 2655.
16. R. M. MARTIN, *Phys. Rev.* **B6** (1972) 4546.
17. G. ARLT and G. R. SCHODDER, *J. Acoust. Soc. Amer.* **37** (1965) 384.
18. D. J. REED and B. J. WUENSCH, *J. Amer. Ceram. Soc.* **63** (1980) 88.
19. Y. OISHI and W. D. KINGERY, *J. Chem. Phys.* **33** (1960) 480.
20. A. E. PALADINO and W. D. KINGERY, *ibid.* **37** (1962) 957.
21. J. D. HONG and R. F. DAVIS, *J. Amer. Ceram. Soc.* **63** (1980) 546.
22. M. LE GALL, B. LESAGE and J. BERNARDINI, *Phil Mag.* **A70** (1994) 761.
23. G. H. KUCERA, I. BLOOM and M. F. ROCHE, *J. Electrochem. Soc.* **133** (1986) 1996.
24. G. LUCAZEAU, J. R. GAVARRI and A. J. DIANOUX, *J. Phys. Chem. Solids* **48** (1987) 57.
25. N. D. PATEL and P. S. NICHOLSON, *Solid State Ionics* **22** (1987) 305.
26. A. S. NOWICK and B. S. BERRY, "Anelastic Relaxation in Crystalline Solids" (Academic Press, New York, 1972) pp. 454–461.

Received 23 May
and accepted 23 October 1996